The Spine Journal 25 (2025) 1951–1963

Clinical Study

Normalizing spinal cord compression measures in degenerative cervical myelopathy

Sandrine Bédard, MSc[a,#], Jan Valošek, PhD[a,b,c,d,#], Maryam Seif, PhD[e,f], Armin Curt, MD[e], Simon Schading-Sassenhausen, MSc[e], Nikolai Pfender, MD[e], Patrick Freund, MD, PhD[e,f,g], Markus Hupp, MD[e], Julien Cohen-Adad, PhD[a,b,h,i,*]

[a] *NeuroPoly Lab, Institute of Biomedical Engineering, Polytechnique Montreal, 2500 Chem. de Polytechnique, Montréal, H3T 1J4, Québec, Canada*

[b] *Mila - Quebec AI Institute, 6666 Rue Saint-Urbain, Montréal, H2S 3H1, Québec, Canada*

[c] *Department of Neurosurgery, Faculty of Medicine and Dentistry, Palacký University Olomouc, 775 15, Hněvotínská 976/3, Nová Ulice, 779 00 Olomouc, Czechia*

[d] *Department of Neurology, Faculty of Medicine and Dentistry, Palacký University Olomouc, 775 15, Hněvotínská 976/3, Nová Ulice, 779 00 Olomouc, Czechia*

[e] *Spinal Cord Injury Center, Balgrist University Hospital, University of Zurich, Forchstrasse 340, 8008 Zurich, Switzerland*

[f] *Department of Neurophysics, Max Planck Institute for Human Cognitive and Brain Sciences, Stephanstrae 1a, 04103 Leipzig, Germany*

[g] *Wellcome Trust Centre for Neuroimaging, Queen Square Institute of Neurology, University College London, 12 Queen Square, London WC1N 3AR, United Kingdom*

[h] *Functional Neuroimaging Unit, CRIUGM, University of Montreal, 4545, Queen Mary Road, Montreal, H3W 1W4, Quebec, Canada*

[i] *Centre de recherche du CHU Sainte-Justine, Université de Montréal, 4545 Chem. Queen Mary, Montréal, H3W 1W4, Quebec, Canada*

Received 9 September 2024; revised 6 January 2025; accepted 22 March 2025

Abstract

BACKGROUND CONTEXT: Accurate and automatic MRI measurements are relevant for assessing spinal cord compression severity in degenerative cervical myelopathy (DCM) and guiding treatment. The widely-used maximum spinal cord compression (MSCC) index has limitations. Firstly, it normalizes the anteroposterior cord diameter by that above and below the compression but does not account for cord size variation along the superior-inferior axis, making MSCC sensitive to compression level. Secondly, cord shape varies across individuals, making MSCC sensitive to this variability. Thirdly, MSCC is typically calculated by an expert-rater from a single sagittal slice, which is time-consuming and prone to variability.

PURPOSE: This study proposes a fully automatic pipeline to compute MSCC.

DESIGN: We developed a normalization strategy for traditional MSCC (anteroposterior diameter) using a healthy adults database (n = 203) to address cord anatomy variability across individuals and evaluated additional morphometrics (transverse diameter, area, eccentricity, and solidity).

PATIENT SAMPLE: DCM patient cohort of n = 120.

OUTCOME MEASURES: Receiver operating characteristic (ROC) and area under the curve (AUC) were used as evaluation metrics.

METHODS: We validated the method in a mild DCM patient cohort against manually derived morphometrics and predicted the therapeutic decision (operative/conservative) using a stepwise binary logistic regression incorporating demographics and clinical scores.

RESULTS: The automatic and normalized MSCC measures correlated significantly with clinical scores and predicted the therapeutic decision more accurately than manual MSCC. Significant

FDA device/drug status: Not applicable.

Author disclosures: ***SB:*** Nothing to disclose. ***JV:*** Nothing to disclose. ***MS:*** Nothing to disclose. ***AC:*** Nothing to disclose. ***SS-S:*** Nothing to disclose. ***NP:*** Nothing to disclose. ***PF:*** Nothing to disclose. ***MH:*** Nothing to disclose. ***JC-A:*** Nothing to disclose.

*Corresponding author: NeuroPoly Lab, Institute of Biomedical Engineering, Polytechnique Montreal, 2500 Chem. de Polytechnique, Montréal, QC, H3T 1J4, Canada. Tel.: +1 (514) 340-4711.

E-mail address: julien.cohen-adad@polymtl.ca (J. Cohen-Adad).

[#] Shared cofirst authorship - authors contributed equally.

https://doi.org/10.1016/j.spinee.2025.03.012

predictors included upper extremity sensory dysfunction, T2w hyperintensity, and the proposed MRI-based measures. The model achieved an area under the curve of 0.80 in receiver operating characteristic analysis.

CONCLUSION: This study introduced an automatic method for computing normalized measures of cord compressions from MRIs, potentially improving therapeutic decisions in DCM patients. The method is open-source and available in Spinal Cord Toolbox v6.0 and above.

Keywords: DCM; degenerative cervical myelopathy; MRI; magnetic resonance imaging; Image analysis; MSCC; Maximum spinal cord compression; Spinal cord

Introduction

Morphometric measures computed from structural magnetic resonance imaging (MRI) scans are often used to evaluate the severity of spinal cord compressions [1–3]. While morphometric measures demonstrated the potential to predict the progression of degenerative cervical myelopathy (DCM) [4,5] and to guide therapeutic strategy [6–8], they currently fail to show a clear association with the clinical status in DCM. Moreover, these measures present considerable variability due to anatomical differences along the spinal cord and across individuals, currently limiting their clinical application. Clinical guidelines recommend surgical decompression for moderate-to-severe DCM; however, the optimal timing of surgery in mild DCM remains uncertain [9]. Improving the morphometric measures by addressing their limitations outlined below could further help guide therapeutic decision-making, especially in mild compression where clinical guidelines are less clear and clinical scores show poor sensitivity.

Variations in spinal cord anatomy along the superior-inferior axis within a single individual lead to different morphometric measures between levels. For example, spinal cord measures have highest values at C5 vertebral level, while the cord is smaller in other cervical segments [10–12]. Maximum spinal cord compression (MSCC) is a common index providing compression severity normalized by using the non-compressed levels above and below the compression site [13]. However, traditional MSCC uses only the anteroposterior (AP) diameter and does not consider the varying spinal cord anatomy along the spinal cord, which can lead to inaccuracies in the assessment of compression severity, as the measures may not reflect the true pathology extent. For instance, if a compression occurs at the cervical enlargement (around C5 vertebral level), the MSCC may be underestimated because the levels above and below the compression site are smaller than the cervical enlargement. Analogously, if the compression happens right below the cervical enlargement, the opposite can happen: the MSCC would be overestimated. Additionally, the MSCC is often calculated from manual measures on a single sagittal slice which is time-consuming and prone to variability between raters.

Inter-subject variability is also a confounder of MSCC values. Values could be biased in terms of differences in age, sex, and body size (ie, weight, height) between individuals. For instance, a significantly smaller spinal cord area is consistently reported in females relative to males [12,14,15]. Similarly, age-related changes in spinal cord size and shape can impact spinal cord morphometrics and may require different normalization strategies for different age groups [15]. Previous studies proposed different normalization strategies to mitigate this variability, including normalizing to age-matched healthy control [16] and taking into account confounding variables such as age and brain volume [14,15,17]. However, an age- and sex-matched healthy control cohort is not always available, and measures like brain volume are not commonly accessible within spinal cord studies.

Thus, this study aimed to improve the accuracy and clinical utility of spinal cord compression morphometric measures addressing the effects of intra-subject (ie, varying spinal cord anatomy along the spinal cord) and inter-subject (ie, related to age and sex). We developed a method to automatically compute MSCC and extended it to include additional morphometric measures such as transverse (RL) diameter, cross-sectional area (CSA), eccentricity, and solidity. Furthermore, we implemented a MSCC normalization using a cohort of healthy individuals to account for the varying anatomy along the spinal cord. We validated this approach in a large cohort of mild DCM patients (n = 120) against manually-derived morphometric measures to predict the therapeutic decision in the cohort. We hypothesize that automatic measures will better reflect therapeutic decisions than manual ones. Having reliable and objective measures has the potential to provide new insights into optimizing therapeutic decision-making in mild DCM cases, where uncertainty often complicates clinical management. The proposed method is available as part of the open-source software Spinal Cord Toolbox (SCT) v6.0 and above [18].

Materials and methods

Normalization of morphometric measures

Automatic MSCC computation

Spinal cord morphometrics were calculated with Spinal Cord Toolboox (v6.0) via the *sct_compute_compression* function. We automated the MSCC computation and refer

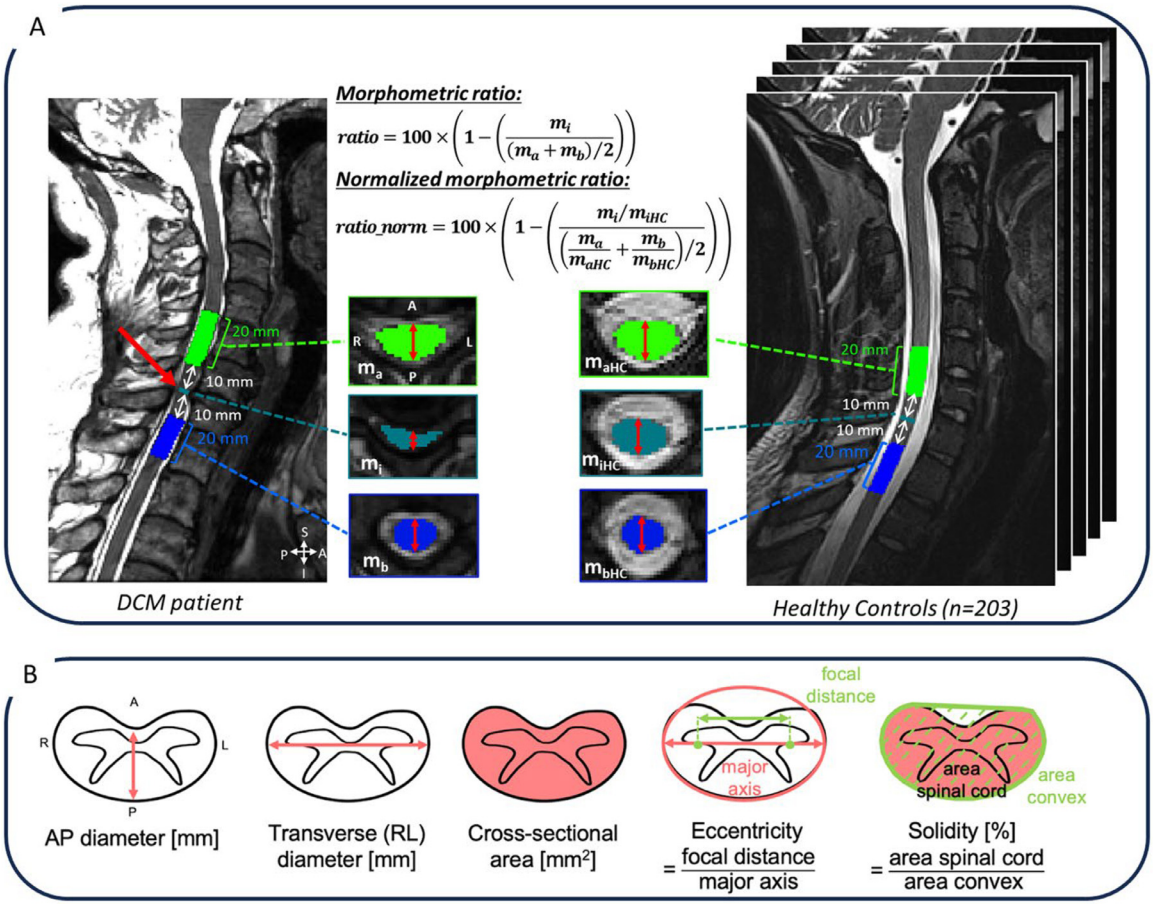

Fig. 1. **(A)** Morphometric ratio and normalized morphometric ratio. The morphometric ratio is computed based on the metric (here AP diameter is shown) at the compression site (m_i), 10 mm above (m_a) and 10 mm below (m_b) the compression and averaged along a 20 mm extent of the spinal cord in patients and healthy controls. Normalized morphometric ratio (ratio_norm) is computed by dividing each metric (m_x) by the corresponding value averaged across healthy controls (m_{aHC} respectively m_{bHC}). **(B)** Morphometric measures used to compute morphometric ratios and normalized morphometric ratios. Adapted from [12].

to these metrics normalized with noncompressed healthy spinal cord levels above and below as *morphometric ratios*. Fig. 1 presents an overview of the automatic morphometric ratios' computation. Given that cord compression typically affects more than one MRI axial slice, and compression sites are commonly located near the intervertebral discs, we did not use the spinal cord metrics of the entire vertebral levels above and below the compression site. Instead, we averaged the metrics at a 10 mm distance above and below the compression site over 20 mm length of the spinal cord. If multiple compressions are present, we use 10 mm above the most upper compression, and 10 mm below the lowest compression site to ensure that "noncompressed" levels are used for the normalization. We chose an extent of 20 mm to approximate level length, and a 10 mm distance to reliably select only noncompressed areas [11]. The extent and distance were specified as input arguments of the *sct_compute_compression* function.

Normalization with healthy controls

To account for variability caused by anatomical differences along the spinal cord, aiming to reduce intra-subject variability, the normative morphometrics measures were additionally computed on a database of healthy adult volunteers (n = 203) in the PAM50 spinal cord template anatomical dimensions (Fig, 1A) [11,12]. Next, healthy morphometrics were used to normalize the morphometric ratios for a given patient as illustrated in Fig. 1. To account for the influence of sex and age on the morphometric measures, aiming to reduce inter-subject variability, we implemented an option for the user to filter healthy adult volunteers based on sex (males vs females) and a specific age range (eg, 40-50 y.o.).

Morphometric measures to characterize spinal compression

We implemented the normalization approach for several morphometric measures provided by SCT: 1) AP diameter, 2) RL diameter, 3) CSA, 4) eccentricity, and 5) solidity. Briefly, eccentricity reflects how circular the spinal cord's shape is, while solidity reflects its convexity. A detailed description of individual measures can be found in [12].

The *sct_compute_compression* function requires a spinal cord segmentation mask, vertebral labels, and a file with identified compression sites as inputs. It outputs a CSV file

with computed metrics ratios for each compression site. A tutorial on how to get the labels and use *sct_compute_compression* is available at: https://spinalcordtoolbox.com/user_section/tutorials/shape-analysis/normalize-morphometrics-compression.html.

Validation in patients with cord compression

Participants

In this study, 120 DCM patients were recruited at Balgrist University Hospital (Zurich, Switzerland) between October 2016 and December 2022. The research received approval from the regional ethical review board (Kantonale Ethikkommission Zurich, KEK-ZH 2012-0343, BASEC Nr. PB_2016-00623), and is registered (http://www.clinicaltrials.gov). The execution of the study adhered to the ethical guidelines set forth by the World Medical Association's Declaration of Helsinki, which pertains to human experimentation. Prior to their inclusion in the study, all participants gave their informed consent.

Inclusion criteria: cervical spinal stenosis on the T2-weighted (T2w) MRI; at least one clinical symptoms and sign consistent with DCM [3] (ie, pain, sensory or motor deterioration in the upper or lower limbs, gait or bladder dysfunction); age 18-80 years. Patients suffering from a competing neurological disease with a potential bias to clinical and neurophysiological assessments were excluded. Additional exclusion criteria: MRI contraindications, epileptic seizures, mental illness, severe medical illness and pregnancy. Previous spine surgery was not considered as an exclusion criterion. For more details, the patient population was described previously [19–21].

Clinical assessment

Neurological status and functional impairment were assessed with the following scores:

1. Modified Japanese Orthopedic Scale (mJOA, max. 18 points) and its subscores upper extremity sensory dysfunction, lower extremity motor dysfunction, upper extremity motor dysfunction and bladder dysfunction [22].
2. American Spinal Injury Association (ASIA)/Graded Redefined Assessment of Strength, Sensibility, and Prehension (GRASSP) subscores [23,24]: the upper-extremity light-touch score, the upper-extremity pin prick score (cervical pin prick score), monofilament testing of dorsal hand sensation (monofilament sensation score), upper extremity motor score and lower extremity motor score.

Moreover, the following clinical information was obtained from MRI: level of maximal spinal cord compression, number of stenotic segments, and presence of T2w hyperintensity (0: no, 1: yes), which includes diffuse T2 hyperintensity, cystic lesions, and "snake eyes", within the spinal cord.

Therapeutic decision

Patients were treated either conservatively or operatively. The treatment decision was made by spine surgeons at the Balgrist University Hospital, taking into account the patient's clinical condition, pain severity (assessed clinically, see section *Clinical assessment*), MRI findings, electrophysiological assessments. These decisions were guided by the recommendations outlined in [9]. A shared treatment decision was made between the spine surgeon and the informed patient. None of the patients assigned for operation had to be refused from operation due to their clinical condition.

MRI acquisition

MRI data was obtained on a 3T scanner (Siemens MRI SkyraFit and MRI Prisma, Erlangen, Germany), using the body transmit coil and the product 16-channel receive head/neck coil. An MRI compatible cervical collar was used to reduce involuntary neck motion. The axial T2w scans were acquired with the following MR parameters: TE of 93 ms, TR of 3600 ms, slice thickness of 3 mm, flip angle of 150°, field-of-view of 160 mm, bandwidth of 284 Hz/px, base resolution of 320, phase resolution of 80%, in-plane resolution of 0.5×0.5 mm^2, and GRAPPA = 2. The sagittal T2w scans were acquired with the following MR parameters: TE of 87 ms, TR of 3760 ms, slice thickness of 2.5 mm, flip angle of 160°, field-of-view of 220 mm, bandwidth of 260 Hz/px, base resolution of 384, phase resolution of 75 %, spatial resolution of 0.6×0.6 mm^2.

MRI analysis (manual)

The spinal cord and spinal canal were manually measured in axial T2w images on each cervical level. The adapted spinal canal occupation ratio (aSCOR) was calculated at the level of compression as the ratio of the spinal cord area divided by the spinal canal area multiplied by 100 [21,25] and adapted MSCC (aMSCC) calculated as the ratio of spinal cord CSA in the compressed segment divided by the CSA at C2 vertebral level.

MRI analysis (automatic)

Automatic processing of the MRI was performed using SCT v6.0 [18] and the dcm-metric-normalization pipeline (https://github.com/sct-pipeline/dcm-metric-normalization/releases/tag/r20230222) and is illustrated in Fig. 2. For each participant, intervertebral disc labels were obtained from the sagittal T2w image using *sct_label_vertebrae* [26], and the spinal cord was segmented on the axial T2w image using *sct_deepseg_sc* [27] (Fig. 2A). The intervertebral discs and spinal cord segmentations were visually assessed and manually corrected when necessary. Then, the sagittal T2w image was resampled to the axial T2w image by

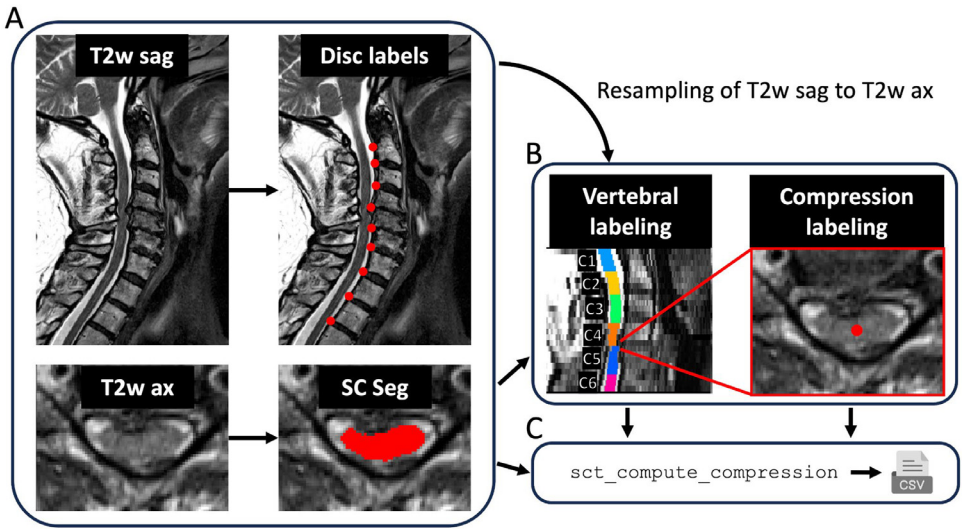

Fig. 2. Automatic processing pipeline. Intervertebral discs were obtained for the sagittal T2w image, and the spinal cord was segmented on the axial T2w image **(A)**. Then, the sagittal T2w image was resampled to the axial T2w images to bring the intervertebral discs from the sagittal to the axial T2w scan to label the axial spinal cord segmentation **(B)**. Spinal cord compression sites were manually labeled, and morphometric ratios and normalized morphometric ratios were automatically computed using the *sct_compute_compression* function **(C)**.

sct_register_multimodal -identity 1 [11] to bring sagittal intervertebral discs to the axial scan and to label the axial spinal cord segmentation (Fig. 2B). The compression sites were manually identified on the axial T2w images based on the provided clinical information (Fig. 2B). Finally, the *sct_compute_compression* function, introduced in this study, was used to automatically compute morphometric ratios and normalized morphometric ratios (section *Morphometric measures to characterize spinal compression*) (Fig. 2C). To mitigate the differences in morphometrics between sex when computing the normalized morphometric ratios, we matched healthy controls for sex. We did not match for age as the existing normative database contains predominantly young subjects [12]; see the Discussion section for details. We computed both morphometric ratios and normalized morphometric ratios of AP diameter, RL diameter, CSA, eccentricity, and solidity. Note that either manual or automatic scores were available to the clinician for the treatment decision making.

Statistics

Statistical analysis was performed with SciPy v1.6.3 and scikit-learn v0.23.2 Python libraries. Descriptive statistics including mean and standard deviation (SD) were provided. The Spearman correlation was performed among all available regressors (as provided in Table 1) between continuous variables. Phi coefficient was computed across dichotomous variables, and the point-biserial correlation was computed across continuous and dichotomous variables. Dichotomous variables included sex, previous surgery, T2w hyperintensity and therapeutic decision. We did not correct for multiple comparisons when computing correlations since the purpose was exploratory and the number of regressors is considered in the subsequent multivariate regression analysis.

To compare the manual vs automatic morphometric ratios, we used Spearman's correlation. We compared how both automatic and manual ratios correlate with clinical scores and how they predict the therapeutic decision.

Correlation between manual, automatic and normalized morphometrics. First, we computed the Spearman's correlation coefficient (ρ) between the manual morphometric measures (aSCOR and aMSCC), and automatic (ie, normalized and not-normalized) morphometric ratios. As aSCOR and aMSCC were computed using the CSA, we only compared them with CSA and normalized CSA morphometric ratios.

Prediction of therapeutic outcome. To validate the automatic computation of morphometric ratios, we created a model to predict the therapeutic decision (conservative: 0, operative: 1) using a stepwise binary logistic regression. The dependent variable was the therapeutic decision. The independent variables included demographics, clinical data, clinical scores, automatic morphometric ratios, and manual morphometric measures as detailed in Table 1.

First, we proceeded to a stepwise logistic regression with p-value=0.05 as the level of significance. A binary logistic regression was computed using the resulting significant variables of the stepwise regression. The model was validated using a 10-fold cross-validation. The receiver operating characteristic (ROC) area under the curve (AUC), and accuracy were used as performance metrics, computed during the 10-fold cross-validation. We repeated the stepwise binary logistic regression using the normalized morphometric ratios instead, leading to two different models. If the participant's maximum level of compression was not included in the axial field-of-view, the participant was excluded from the analysis.

Table 1
Descriptive statistics of demographics, clinical data, clinical scores, and morphometrics data

Demographics		
Age	55.28±12.80	
Sex (M: male/F: female)	M: 64% F: 36%	
Height (m)	1.70±0.10	
Weight (kg)	74.93±14.17	
Clinical data		
Previous surgery (yes/ no)	6%	94%
Therapeutic decision (conservative/operative)	40%	60%
T2w hyperintensity (yes/no)	38%	62%
Number of stenoses	2.09±0.97	
Maximum level of compression	C3/C4: 17% C4/C5: 23% C5/C6: 52% C6/C7: 8%	
Clinical scores		
mJOA (max. 18 points)	15.89±1.84	
mJOA upper extremity motor subscore (max 5 points)	4.54±0.67	
mJOA lower extremity motor subscore (max 7 points)	6.49±0.80	
mJOA upper extremity sensory subscore (max 3 points)	2.18±0.64	
mJOA bladder function subscore (max 3 points)	2.68±0.58	
Monofilament sensation score (max 24 points)	21.78±2.80	
Cervical light touch score (max 28 points)	25.83±3.16	
Cervical pin prick score (max 28 points)	25.16±3.84	
Upper extremity motor score ASIA (max 50 points)	49.34±1.40	
Lower extremity motor score ASIA (max 50 points)	49.58±1.51	
Morphometric ratios (automatic, normalized)		
AP diameter ratio (%)	18.51±11.27	
AP diameter ratio normalized (%)	17.20±9.96	
CSA ratio (%)	18.42±15.36	
CSA ratio normalized (%)	20.38±12.81	
RL diameter ratio (%)	−5.40±12.64	
RL diameter ratio normalized (%)	0.45±9.42	
Eccentricity ratio (%)	−8.29±4.91	
Eccentricity ratio normalized (%)	−4.93±3.80	
Solidity ratio (%)	5.06±5.56	
Solidity ratio normalized (%)	4.48±4.98	
Morphometric ratios (manual)		
aSCOR (%)	75.52±13.16	
aMSCC (%)	100.57±17.38	

Quantitative variables are represented as mean±SD while categorical variables are presented as % in each category.

Results

Descriptive characteristics

A total of 100 DCM patients (mean ± SD age: 55.28 ± 12.80, 64 males) had a complete dataset (ie, MRI and clinical examination). The cohort presents mild DCM (mJOA>14) with mostly sensory deficits. The maximum level of compression was predominantly (52 % of patients) at the C5/C6 intervertebral disc level. The average number of stenoses per patient was 2.09 ± 0.97. Detailed demographics and descriptive statistics for all available regressors are provided in Table 1.

Correlations between morphometrics and clinical scores

The correlation matrix across all variables is presented in the supplementary materials Fig. S1. Some correlations are described in the following.

mJOA and automatic morphometric ratios

Correlations between CSA ratio, CSA ratio normalized, AP diameter ratio, AP diameter ratio normalized, RL diameter ratio and RL diameter ratio normalized were significant with motor dysfunction of lower extremities and upper extremities (mJOA lower extremity motor subscore: $-0.33<\rho<-0.22$, and mJOA upper extremity motor subscore: $-0.36<\rho<-0.19$). The mJOA correlated significantly with AP diameter ratio, CSA ratio and CSA ratio normalized ($-0.29<\rho<-0.22$).

ASIA and automatic morphometric ratios

The upper extremity motor score ASIA correlated with CSA ratio ($\rho=-0.25$, p-value=0.013) and RL diameter ratio ($\rho=-0.24$, p-value=0.015). The lower extremity motor score ASIA correlated with AP diameter ratio ($\rho=-0.23$, p-value=0.024), CSA ratio ($\rho=-0.31$, p-value=0.013), CSA ratio normalized ($\rho=-0.23$, p-value=0.021), and RL diameter ratio ($\rho=-0.22$, p-value=0.03). The cervical light touch score correlated with CSA ratio ($\rho=-0.18$) and CSA ratio normalized ($\rho=-0.18$).

mJOA and ASIA and manual morphometric ratios

aSCOR correlated significantly with mJOA lower extremity motor subscore ($\rho=-0.28$). aMSCC correlated with the cervical pin prick score ($\rho=0.2$).

Correlation between manual, automatic, and normalized morphometrics

Fig. 3 presents the Spearman's correlation and scatter plots between the manual morphometric ratios performed by physicians (aSCOR, aMSCC) and proposed automatic morphometric ratios (CSA ratio and CSA ratio normalized).

Predicting therapeutic decision

Using the available regressors described in Table 1, we tested if the therapeutic decision of the DCM cohort (operative/conservative) could be predicted using a stepwise binary logistic regression. We developed two models: (1) without normalization of the automatic morphometric ratios and (2) with normalization of the automatic morphometric ratios.

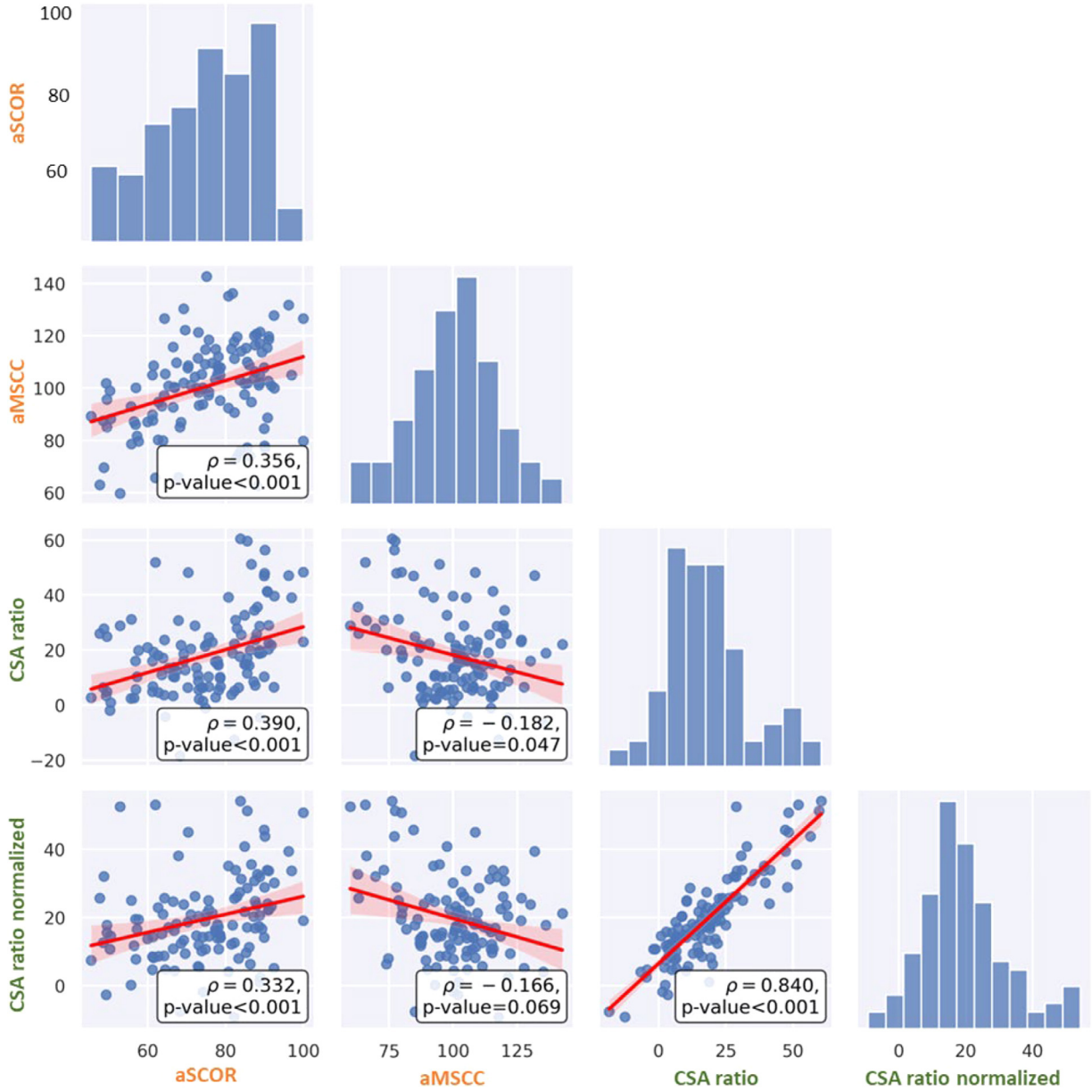

Fig. 3. Spearman's correlation between manual measures (aSCOR, aMSCC) in orange, and automatic morphometric ratios (CSA ratio in %, CSA ratio normalized in %) in green. Red lines show the linear regression fit with confidence intervals. Histograms show the distribution of each variable.

Table 2
Logistic regression with selected parameters from the stepwise regression

1. No Normalization					
	Coef.	***STD.Err.***	***z-score***	**p-*value***	***[0.025 0.975]***
mJOA upper extremity sensory subscore	−0.89	0.19	−4.63	<0.0001	−1.27 −0.52
CSA ratio	0.05	0.02	2.79	0.01	0.02 0.09
T2w hyperintensity	1.09	0.54	2.02	0.04	0.03 2.14
2. Normalization of automatic ratios					
	Coef.	***STD.Err.***	***z-score***	**p-*value***	***[0.025 0.975]***
mJOA upper extremity sensory subscore	−0.96	0.22	−4.42	<0.0001	−1.39 −0.54
CSA ratio normalized	0.05	0.02	2.49	0.01	0.01 0.010
T2w hyperintensity	1.21	0.53	2.27	0.02	0.17 2.25

Coef., coefficient; STD Err, standard error of coefficient.

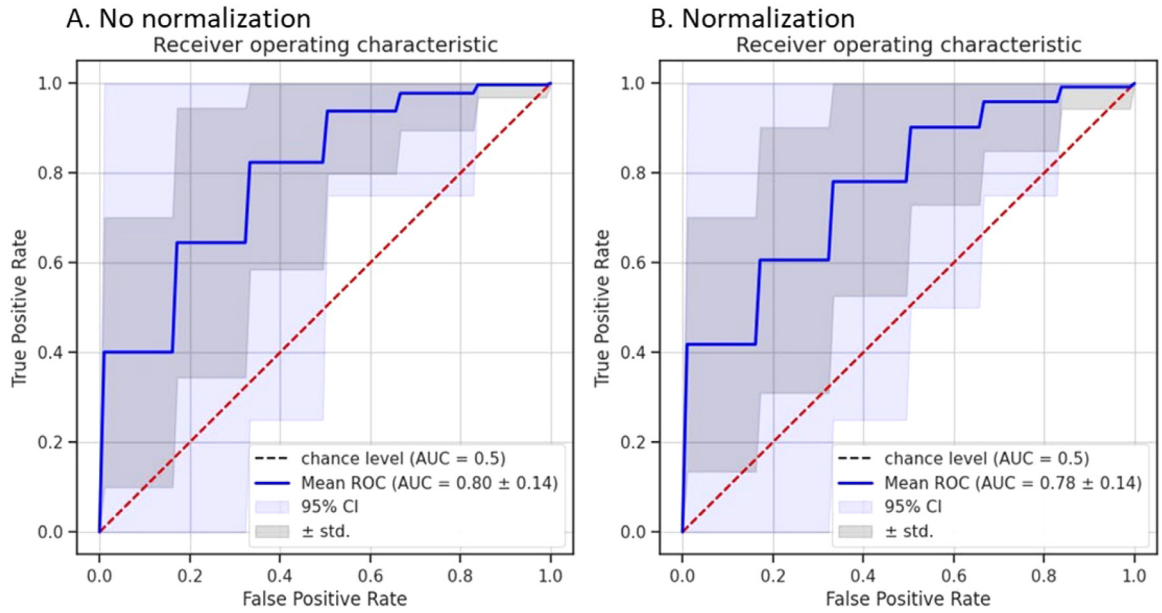

Fig. 4. ROC curve of logistic binary regression to predict therapeutic decision using a 10-fold cross-validation without normalization **(A)** and with normalization **(B)**. Mean ROC curve, 95% confidence interval (CI) and SD are shown.

Table 2 presents the logistic regressions with the significant predictors (p-value<0.05) from the stepwise regression without normalization (model 1) and with normalization (model 2). The resulting ROC curves are presented in Fig. 4 without normalization (Fig. 4A) and with normalization (Fig. 4B). The model without normalization yielded an accuracy of 0.684±0.128 while the accuracy was of 0.661±0.130 with normalization. CSA ratio (model 1) and CSA ratio normalized (model 2) were significant predictors in addition to T2w hyperintensity and the upper extremity sensory subscore.

Discussion

We introduced an automatic method to quantify cord compression from clinical MRI scans. We extended the traditional MSCC (based on AP diameter) with further morphometric measures (RL diameter, CSA, eccentricity, and solidity), and added a normalization across healthy controls to better account for variability in the spinal cord anatomy along the superior-inferior axis as an inter-individual confounder. Validation on a cohort of mild DCM patients showed that the mJOA upper extremity sensory subscore, CSA ratio, CSA ratio normalized, and T2w hyperintensity were significant predictors of the therapeutic decision leading to an AUC of 0.80 (without normalization, model 1) and 0.78 (with normalization, model 2), respectively, while manual anatomic metrics (ie, aSCOR and aMSCC) did not predict the therapeutic decision.

Correlations between morphometrics and clinical scores

The automatically computed MRI morphometric ratios significantly correlated with clinical scores (mJOA and CSA morphometric ratio: ρ=−0.29, p-value=0.004), while the manual MRI morphometrics (ie, aSCOR and aMSCC), failed to show any correlation. Previous studies also reported no correlation between manual MRI morphometrics and mJOA [28−30], or correlation for some morphometrics (compression ratio, maximum canal compression, and MSCC) with mJOA [31,32]. This could be caused by several factors, including differences in cohort sizes and inclusion/exclusion criteria, variability in scanner field strengths (1.5T vs 3.0T) and sequences used (axial vs sagittal; T1w vs T2w), and intra- and inter-rater variability in manual measurements. These findings are in line with previous reports, demonstrating that the extent of spinal canal stenosis often does not completely explain the disease severity and progression [33−35]. While cord compression is one of the driving factors in pathophysiology of DCM, other contributing factors are still insufficiently understood [36−38].

Moreover, although mJOA is currently the widely accepted clinical score for assessing DCM patients, it has poor sensitivity, especially in mild DCM [3]. For example, the minimum reported clinically meaningful change in mJOA is 2 points [3] which is within the mild compression range (mJOA > 14, as observed in our cohort: 15.89 ± 1.84) [3]. This reduces the ability of mJOA to capture subtle variations in compression severity.

Comparison of manual vs automatic MRI measures

When assessing the relationship between the automatic and manual morphometric ratios, we found that the correlation of aMSCC with CSA ratio and CSA ratio normalized was only of ρ=−0.182 (p-value=0.047) and ρ=−0.166 (p-

value=0.069), respectively (Fig. 3). Given that aMSCC is calculated as the area at the maximum compressed level divided by the area at the C2 vertebral level, a higher agreement with the automatic morphometric ratios was expected. Moreover, we found that aSCOR (calculated as the ratio of the spinal cord area divided by the spinal canal area) had a stronger correlation with the CSA ratio and the CSA ratio normalized (ρ=0.395 and ρ=0.325, respectively) than aMSCC.

In the current study, the model identified CSA and normalized CSA morphometric ratios as significant predictors of the therapeutic decision, while manual measures (aSCOR nor aMSCC) were not significant predictors (Table 2), reflecting that our automatic measures better align with the clinicians' anatomical MRI assessment.

To compute the automatic morphometric measures, we utilized tools from the open-source software SCT, including *sct_label_vertebrae*, *sct_deepseg_sc*, and *sct_register_multimodal*. These tools were validated in previous studies, in controls and various pathological populations [11,18,26,39]. Additionally, all automatic outputs were subjected to rigorous visual quality control, with manual corrections applied in cases of errors (eg, over/under segmentation) [40]. This combined approach of automatic processing and manual validation ensures the accuracy and robustness of the derived morphometric measures.

Only a few studies have used automatic or semi-automatic shape measures to compute spinal cord morphometrics [5,16,17,41–43]. Previous studies manually measured the AP diameter on a single mid-sagittal slice [1,30,32,35,44,45]. The mid-sagittal slice may not correspond precisely to the middle of the spinal cord due to patient scoliosis and/or sequence positioning and may not capture the full extent of the compression as it does not consider the para-sagittal slices. In contrast, our automatic measures consider all the slices to compute the morphometrics along the spinal cord centerline, leveraging the segmentation of the spinal cord. These segmentations undergo a robust visual validation process, with manual corrections applied where necessary, ensuring their accuracy. Additionally, measuring the morphometrics manually is time-consuming, especially in large cohorts, and potentially prone to inter-rater variability [13,31]. Indeed, a study comparing manually vs automatically derived morphometrics (CSA, compression ratio, AP diameter, and RL diameter) showed higher inter-rater reliability for the automatically computed morphometrics [16].

As the computation of MSCC only with AP diameter does not necessarily reflect the compression severity, and might poorly quantify lateral compression [35], we extended the MSCC to other shape metrics, likely increasing the ability to detect and characterize various types of compressions [46]. In fact, we found that morphometric ratios based on CSA were identified as significant predictors of the therapeutic decision, while morphometric ratios based on AP diameter were not. However, we did not stratify the cohort by compression type, which may have influenced the overall correlation and selected predictor."

Some studies directly used the AP diameter or CSA in their analysis without normalization with healthy levels above and below the compression sites [4,16,42,43,47]. Spinal cord morphometry has a large inter-subject variability, especially for CSA, AP and RL diameters [11,12,14] and between males and females [12,14,15,48–50]. This suggests the need for normalization using healthy levels in cross-sectional studies.

Predicting therapeutic decision

The analysis of 100 participants with a complete dataset identified T2w hyperintensity, CSA ratio, CSA ratio normalized and the upper extremity sensory subscore as predictors guiding the decision for surgical intervention (Table 2) with an AUC of 80%.

While AUC is a valuable metric in summarizing overall model performance, including sensitivity and specificity, it does not reflect the model's behavior at specific decision thresholds or the balance between accurate predictions and misclassifications. Also note that the proposed model was based on patients with mild DCM and might not be appropriate for moderate or severe DCM. Other comorbidities should be taken into account when making that therapeutic decision.

Therapeutic decision is based on the patients' symptoms, and clinical, neurophysiological, and radiological assessments. As up to 62 % of DCM patients will deteriorate if treated conservatively, the standard of care for moderate-to-severe DCM is surgical decompression [9]. However, the optimal timing of surgery is uncertain with no clear cut-off, and some DCM patients further deteriorate even after surgery. In our analysis, we found that the therapeutic decision was based on the automatic anatomical MRI measures and T2w hyperintensity. When making the therapeutic decision, the neurosurgeons had access to clinical scores, anatomical MRI and electrophysiological assessment. Note that electrophysiological assessment was not included in this study since it was not performed on all the patients. No morphometric ratios (manual or automatic) were provided. The therapeutic decision remains multifactorial, which may explain the variability in the significant predictors when changing the included participants in the analysis [29]. This suggests the need for large multicenter repositories aggregating MRI and clinical data across different demographics and clinical settings. Having more robust structural markers can be used to monitor myelopathic progression [5] and help with clinical decision making.

Hilton et al [29] investigated the factors in current practice that influence the decision to operate in 39 DCM patients, and concluded that only the compression ratio was a significant predictor of the decision to operate.

Impact of across-subject normalization

We presented two different models, with and without normalization of morphometric ratios, predicting the therapeutic decision in a cohort of DCM patients. In both models, the same automatic morphometric ratios were identified as significant predictors and showed comparable AUCs (normalized: 0.78 ± 0.14, not-normalized: 0.80 ± 0.14). Although no clear benefit of this additional normalization was shown, the analysis in this study was on the prediction of the therapeutic decision, while subsequent analysis on clinical outcomes will be of higher clinical interest. The majority of DCM patients in this study had their maximum spinal cord compression located at the C5/C6 level (52 % of patients), which aligns with previous findings [4,47]. This might reduce the overall effect of the normalization as it is designed to be beneficial especially when patients have a maximum level of compression located in different levels.

Additionally, the effect of the normalization might be influenced by different age ranges. The DCM cohort in this study had a mean ± SD age of 55.28 ± 12.80 years old, while the healthy control database had an age of 28.7 ± 5.6 year old.

A significant correlation between the number of stenoses and age (ρ=0.21, p-value=0.034) observed in our study, corresponds with previous findings demonstrating a higher prevalence of spinal cord compression with increasing age [47,51].

Limitations and Perspective

Our model for predicting the therapeutic decision included only morphometric ratios at the maximum level of compression, which may not capture the full extent of pathology, for instance, in multilevel stenosis. We also did not differentiate between types of surgery and did not incorporate spinal canal morphometrics. However, our automatic morphometric ratios can be computed for other compressed levels and for the spinal canal, if spinal canal segmentation is provided.

While most patients suffered from mild DCM and severe medical illness was an exclusion criteria, factors like the patients' detailed health status, whether they can bear the risk of operation and the risk of anesthesia were not collected and have not been taken into account. However, none of the patients assigned for operation had to be refused due to his health status.

The computation of morphometrics directly depends on the quality of the spinal cord segmentation, which can require manual correction (38 % of images had to be manually corrected in this study, which took about 3 minutes per image). In cases of severe spinal cord compression, segmenting the spinal cord becomes more challenging. The introduction of more robust segmentation models will help reduce manual intervention [52–54]. Furthermore, choosing a predefined distance from the compression site for normalization does not consider inter-subject variability of spinal cord length. We filtered healthy controls according to sex when computing normalized morphometric ratios but not based on age, as the existing normative database contains predominantly younger subjects. Other limitations exist for the use of vertebral levels as they do not precisely estimate the spinal levels' location [55–57]. In our pipeline, compression sites need to be manually labeled on the MRI image. Future research could focus on the automatic detection of spinal cord compressions.

Computing morphometrics on anisotropic images with thick slices (3–5 mm) as typically acquired clinically limits the precision of the measurements. Additionally, MRI acquisition in a supine position may fail to accurately depict spinal cord compression associated with weight-bearing, and miss the dynamic compression visible during flexion/extension of the head [58]. A 3D acquisition protocol with isotropic resolution would be relevant to increase the precision of the morphometric computation [40,50]. Inter-scanner, MRI field strength and acquisition sequence variability must also be considered. It can be minimized by using a standardized protocol [50].

Incorporating quantitative MRI biomarkers sensitive to spinal cord tissue integrity and microstructure might help in understanding macrostructural results and the underlying mechanisms of the pathology, especially in patients with mild DCM [17,59–62].

In clinical practice, spinal cord compression, especially in follow up MRIs, is assessed mostly visually and qualitatively by radiologists, the judgement is subject to rater bias. The standard of care for moderate-to-severe DCM is surgical decompression [9]. However, optimal timing of surgery is uncertain, and some DCM patients will deteriorate in the postoperative settings [9]. Having reliable quantitative morphometric measurements of the compression will allow more precise monitoring of cord compression (ie, judgement on worsening cord compression), further aid decision-making in the timing of surgery, and potentially improve patient outcomes. Additionally, this opens the door to comparing with a normal population to quickly assess severity of the compression. Risk factors of deterioration, which are very important to follow closely in mild DCM cases, mentioned by [9] indeed include "circumferential cord compression on axial magnetic resonance imaging (MRI)" which we quantify automatically.

Conclusion

We introduced an automatic pipeline to quantify and characterize spinal cord compression from MRI scans in DCM patients. The output metrics are normalized using a database of healthy adults. We show superior agreement of the automatic morphometric ratios with clinical scores compared to manual measures. Standardized and automatically computed cord morphometrics ensure more precision and accuracy in our ability to detect subtle cord

compression due to traumatic and nontraumatic events. These objective markers have the potential to serve towards better informed therapeutic decisions.

Data and code availability

The dataset of DCM patients is available on request from the corresponding author. The data are not publicly available due to privacy or ethical restrictions.

The data from healthy adults is open-access a part of the Spine Generic Multisubject project and is available here: https://github.com/spine-generic/data-multi-subject/tree/r20230223.

The code used to analyze the DCM cohort is available on GitHub https://github.com/sct-pipeline/dcm-metric-normalization/releases/tag/r20230222.

The normalization method is available through the sct_compute_compression function as part of the Spinal Cord Toolbox (SCT) v6.0 and higher: https://github.com/spinalcordtoolbox/spinalcordtoolbox/tree/6.0.

Ethics

The research received approval from the regional ethical review board (Kantonale Ethikkommission Zurich, KEK-ZH 2012-0343, BASEC Nr. PB_2016-00623), and is registered (www.clinicaltrials.gov). The execution of the study adhered to the ethical guidelines set forth by the World Medical Association's Declaration of Helsinki, which pertains to human experimentation. Prior to their inclusion in the study, all participants gave their informed consent.The open-access healthy adult dataset complied with all ethics regulation, see [50] for more details.

Declaration of competing interest

The authors declare that they have no known competing financial interests or personal relationships that could have appeared to influence the work reported in this paper.

CRediT authorship contribution statement

Sandrine Bédard: Writing – original draft, Visualization, Validation, Software, Methodology, Investigation, Formal analysis, Data curation, Conceptualization. **Jan Valošek:** Writing – original draft, Visualization, Validation, Software, Methodology, Investigation, Formal analysis, Data curation, Conceptualization. **Maryam Seif:** Writing – review & editing, Resources, Funding acquisition. **Armin Curt:** Writing – review & editing, Resources. **Simon Schading-Sassenhausen:** Writing – review & editing, Resources. **Nikolai Pfender:** Writing – review & editing, Resources. **Patrick Freund:** Writing – review & editing, Supervision, Resources, Investigation, Funding acquisition, Data curation. **Markus Hupp:** Writing – review & editing, Resources, Project administration, Investigation, Funding acquisition, Data curation. **Julien Cohen-Adad:** Writing – review & editing, Supervision, Resources, Project administration, Investigation, Funding acquisition.

Acknowledgments

Funded by the Canada Research Chair in Quantitative Magnetic Resonance Imaging [CRC-2020-00179], the Canadian Institute of Health Research [PJT-190258], the Canada Foundation for Innovation [32454, 34824], the Fonds de Recherche du Québec - Santé [322736, 324636], the Natural Sciences and Engineering Research Council of Canada [RGPIN-2019-07244], the Canada First Research Excellence Fund (IVADO and TransMedTech), the Courtois NeuroMod project, the Quebec BioImaging Network [5886, 35450], INSPIRED (Spinal Research, UK; Wings for Life, Austria; Craig H. Neilsen Foundation, USA), Mila - Tech Transfer Funding Program. Supported by the Ministry of Health of the Czech Republic, grant nr. NU22-04-00024. All rights reserved. This project has received funding from the European Union's Horizon Europe research and innovation programme under the Marie Skłodowska-Curie grant agreement No 101107932. MRI measurements were funded by Balgrist Foundation, Zurich, Switzerland. Imaging was performed with the support of the Swiss Center for Musculoskeletal Imaging, SCMI, Balgrist Campus AG, Zurich.

Supplementary materials

Supplementary material associated with this article can be found in the online version at https://doi.org/10.1016/j.spinee.2025.03.012.

References

[1] Liu H, MacMillian EL, Jutzeler CR, Ljungberg E, MacKay AL, Kolind SH, et al. Assessing structure and function of myelin in cervical spondylotic myelopathy. Neurology 2017;89(6):602–10.

[2] David G, Mohammadi S, Martin AR, Cohen-Adad J, Weiskopf N, Thompson A, et al. Traumatic and nontraumatic spinal cord injury: pathological insights from neuroimaging. Nat Rev Neurol 2019;15(12):718–31.

[3] Fehlings MG, Badhiwala JH, Ahn H, Farhadi HF, Shaffrey CI, Nassr A, et al. Safety and efficacy of riluzole in patients undergoing decompressive surgery for degenerative cervical myelopathy (CSM-Protect): a multicentre, double-blind, placebo-controlled, randomised, phase 3 trial. Lancet Neurol 2021;20(2):98–106.

[4] Kadanka Z, Adamova B, Kerkovsky M, Kadanka Z, Dusek L, Jurova B, et al. Predictors of symptomatic myelopathy in degenerative cervical spinal cord compression. Brain Behav 2017;7(9):e00797.

[5] Martin AR, De Leener B, Cohen-Adad J, Kalsi-Ryan S, Cadotte DW, Wilson JR, et al. Monitoring for myelopathic progression with multiparametric quantitative MRI. Toft M, editor PLoS One 2018;13(4):e0195733.

[6] Tetreault L, Palubiski LM, Kryshtalskyj M, Idler RK, Martin AR, Ganau M, et al. Significant predictors of outcome following surgery for the treatment of degenerative cervical myelopathy: a systematic review of the literature. Neurosurg Clin N Am 2018;29(1):115–27.e35.

[7] Tetreault L, Kopjar B, Cote P, Arnold P, Fehlings M. A clinical prediction rule for functional outcomes in patients undergoing surgery

for severe degenerative cervical myelopathy: analysis of an international AOSpine prospective multicentre dataset of 254 subjects. Global Spine J 2016;6(1_suppl):2038–46.
[8] Nouri A, Martin AR, Nater A, Witiw CD, Kato S, Tetreault L, et al. Influence of magnetic resonance imaging features on surgical decision-making in degenerative cervical myelopathy: results from a global survey of AOSpine international members. World Neurosurg 2017 Sep;105:864–74.
[9] Fehlings MG, Tetreault LA, Riew KD, Middleton JW, Aarabi B, Arnold PM, et al. A clinical practice guideline for the management of patients with degenerative cervical myelopathy: recommendations for patients with mild, moderate, and severe disease and nonmyelopathic patients with evidence of cord compression. Global Spine Journal 2017;7(3_supplement):70S–83S.
[10] Sherman JL, Nassaux PY, Citrin CM. Measurements of the normal cervical spinal cord on MR imaging. AJNR Am J Neuroradiol 1990;11(2):369–72.
[11] De Leener B, Fonov VS, Collins DL, Callot V, Stikov N, Cohen-Adad J. PAM50: unbiased multimodal template of the brainstem and spinal cord aligned with the ICBM152 space. Neuroimage 2018;165:170–9.
[12] Valošek J, Bédard S, Keřkovský M, Rohan T, Cohen-Adad J. A database of the healthy human spinal cord morphometry in the PAM50 template space. Imag Neurosci 2024;2:1–15.
[13] Fehlings MG, Rao SC, Tator CH, Skaf G, Arnold P, Benzel E, et al. The optimal radiologic method for assessing spinal canal compromise and cord compression in patients with cervical spinal cord injury. Part II: results of a multicenter study. Spine 1999;24(6):605–13.
[14] Bédard S, Cohen-Adad J. Automatic measure and normalization of spinal cord cross-sectional area using the pontomedullary junction. Front Neuroimaging 2022;1:43.
[15] Papinutto N, Asteggiano C, Bischof A, Gundel TJ, Caverzasi E, Stern WA, et al. Intersubject variability and normalization strategies for spinal cord total cross-sectional and gray matter areas. J. Neuroimaging 2020 Jan 30;30(1):110–8.
[16] Horáková M, Horák T, Valošek J, Rohan T, Koritáková E, Dostál M, et al. Semi-automated detection of cervical spinal cord compression with the Spinal Cord Toolbox. Quant Imaging Med Surg 2022;12 (4):2261–79.
[17] Martin AR, De Leener B, Cohen-Adad J, Cadotte DW, Nouri A, Wilson JR, et al. Can microstructural MRI detect subclinical tissue injury in subjects with asymptomatic cervical spinal cord compression? A prospective cohort study. BMJ Open 2018;8(4):e019809.
[18] De Leener B, Lévy S, Dupont SM, Fonov VS, Stikov N, Louis Collins D, et al. SCT: spinal Cord Toolbox, an open-source software for processing spinal cord MRI data. Neuroimage 2017;145 (Pt A):24–43.
[19] Pfender N, Rosner J, Zipser CM, Friedl S, Vallotton K, Sutter R, et al. Comparison of axial and sagittal spinal cord motion measurements in degenerative cervical myelopathy. J Neuroimaging 2022;32 (6):1121–33.
[20] Hupp M, Pfender N, Vallotton K, Rosner J, Friedl S, Zipser CM, et al. The restless spinal cord in degenerative cervical myelopathy. AJNR Am J Neuroradiol. 2021;42(3):597–609.
[21] Pfender N, Rosner J, Zipser CM, Friedl S, Schubert M, Sutter R, et al. Increased cranio-caudal spinal cord oscillations are the cardinal pathophysiological change in degenerative cervical myelopathy. Front Neurol 2023;14:1217526.
[22] Tetreault L, Kopjar B, Nouri A, Arnold P, Barbagallo G, Bartels R, et al. The modified Japanese Orthopaedic Association scale: establishing criteria for mild, moderate and severe impairment in patients with degenerative cervical myelopathy. Eur Spine J 2017;26(1):78–84.
[23] Kalsi-Ryan S, Riehm LE, Tetreault L, Martin AR, Teoderascu F, Massicotte E, et al. Characteristics of upper limb impairment related to degenerative cervical myelopathy: development of a sensitive hand assessment (Graded Redefined Assessment of Strength, Sensibility, and Prehension Version Myelopathy). Neurosurgery 2020;86 (3):E292–9.
[24] Roberts TT, Leonard GR, Cepela DJ. Classifications In brief: American Spinal Injury Association (ASIA) impairment scale. Clin Orthop Relat Res 2017;475(5):1499–504.
[25] Wolf K, Reisert M, Beltrán SF, Klingler JH, Hubbe U, Krafft AJ, et al. Spinal cord motion in degenerative cervical myelopathy: the level of the stenotic segment and gender cause altered pathodynamics. J Clin Med Res 2021;10(17). https://doi.org/10.3390/jcm10173788.
[26] Ullmann E, Pelletier Paquette JF, Thong WE, Cohen-Adad J. Automatic labeling of vertebral levels using a robust template-based approach. Int J Biomed Imaging 2014;2014:719520.
[27] Gros C, De Leener B, Badji A, Maranzano J, Eden D, Dupont SM, et al. Automatic segmentation of the spinal cord and intramedullary multiple sclerosis lesions with convolutional neural networks. Neuroimage 2019;184:901–15.
[28] Tempest-Mitchell J, Hilton B, Davies BM, Nouri A, Hutchinson PJ, Scoffings DJ, et al. A comparison of radiological descriptions of spinal cord compression with quantitative measures, and their role in non-specialist clinical management. PLoS One 2019;14(7):e0219380.
[29] Hilton B, Tempest-Mitchell J, Davies BM, Francis J, Mannion RJ, Trivedi R, et al. Cord compression defined by MRI is the driving factor behind the decision to operate in Degenerative Cervical Myelopathy despite poor correlation with disease severity. PLoS One 2019;14 (12):e0226020.
[30] Chen G, Li J, Wei F, Ji Q, Sui W, Chen B, et al. Short-term predictive potential of quantitative assessment of spinal cord impairment in patients undergoing French-door laminoplasty for degenerative cervical myelopathy: preliminary results of an exploratory study exploiting intraoperative ultrasound data. BMC Musculoskelet Disord 2020;21(1):336.
[31] Karpova A, Arun R, Davis AM, Kulkarni AV, Mikulis DJ, Sooyong C, et al. Reliability of quantitative magnetic resonance imaging methods in the assessment of spinal canal stenosis and cord compression in cervical myelopathy. Spine 2013;38(3):245–52.
[32] Guo S, Lin T, Wu R, Wang Z, Chen G, Liu W. The pre-operative duration of symptoms: the most important predictor of post-operative efficacy in patients with degenerative cervical myelopathy. Brain Sci 2022;12(8). https://doi.org/10.3390/brainsci12081088.
[33] Golash A, Birchall D, Laitt RD, Jackson A. Significance of CSF area measurements in cervical spondylitic myelopathy. Br J Neurosurg. 2001;15(1):17–21.
[34] Akter F, Kotter M. Pathobiology of degenerative cervical myelopathy. Neurosurg Clin N Am 2018;29(1):13–9.
[35] Nouri A, Martin AR, Mikulis D, Fehlings MG. Magnetic resonance imaging assessment of degenerative cervical myelopathy: a review of structural changes and measurement techniques. Neurosurg Focus 2016;40(6):E5.
[36] Karadimas SK, Gatzounis G, Fehlings MG. Pathobiology of cervical spondylotic myelopathy. Eur Spine J 2015;24(Suppl 2(S2)):132–8.
[37] Karadimas SK, Klironomos G, Papachristou DJ, Papanikolaou S, Papadaki E, Gatzounis G. Immunohistochemical profile of NF-κb/p50, NF-κb/p65, MMP-9, MMP-2, and u-PA in experimental cervical spondylotic myelopathy. Spine (Phila Pa 1976) 2013;38(1):4–10.
[38] Beattie MS, Manley GT. Tight squeeze, slow burn: inflammation and the aetiology of cervical myelopathy. Brain 2011;134(Pt 5):1259–61.
[39] Gros C, De Leener B, Dupont SM, Martin AR, Fehlings MG, Bakshi R, et al. Automatic spinal cord localization, robust to MRI contrasts using global curve optimization. Med Image Anal 2018;44:215–27.
[40] Valošek J, Cohen-Adad J. Reproducible spinal cord quantitative MRI analysis with the spinal cord toolbox. Magn Reson Med Sci 2024;23 (3):307–15.
[41] Martin AR, De Leener B, Cohen-Adad J, Cadotte DW, Kalsi-Ryan S, Lange SF, et al. A novel MRI biomarker of spinal cord white matter

injury: t2*-weighted white matter to gray matter signal intensity ratio. AJNR Am J Neuroradiol 2017 Jun;38(6):1266–73.
[42] Hameed S, Muhammad F, Haynes G, Smith L, Khan AF, Smith ZA. Early neurological changes in aging cervical spine: insights from PROMIS mobility assessment. Geroscience 2024. https://doi.org/10.1007/s11357-023-01050-7.
[43] Filimonova E, Vasilenko I, Kubetsky Y, Prokhorov O, Abdaev M, Rzaev J. Brainstem and subcortical regions volume loss in patients with degenerative cervical myelopathy and its association with spinal cord compression severity. Clin Neurol Neurosurg 2023;233:107943.
[44] Nouri A, Tetreault L, Dalzell K, Zamorano JJ, Fehlings MG. The relationship between preoperative clinical presentation and quantitative magnetic resonance imaging features in patients with degenerative cervical myelopathy. Neurosurgery 2017;80(1):121–8.
[45] Fang Y, Li S, Wang J, Zhang Z, Jiang W, Wang C, et al. Diagnostic efficacy of tract-specific diffusion tensor imaging in cervical spondylotic myelopathy with electrophysiological examination validation. Eur Spine J 2024 Available from:. https://doi.org/10.1007/s00586-023-08111-7.
[46] Kameyama T, Hashizume Y, Ando T, Takahashi A, Yanagi T, Mizuno J. Spinal cord morphology and pathology in ossification of the posterior longitudinal ligament. Brain 1995;118(Pt 1):263–78.
[47] Kovalova I, Kerkovsky M, Kadanka Z, Kadanka Z, Nemec M, Jurova B, et al. Prevalence and imaging characteristics of nonmyelopathic and myelopathic spondylotic cervical cord compression. Spine 2016;41(24):1908–16.
[48] Solstrand Dahlberg L, Viessmann O, Linnman C. Heritability of cervical spinal cord structure. Neurol Genet 2020;6(2):e401.
[49] Engl C, Schmidt P, Arsic M, Boucard CC, Biberacher V, Röttinger M, et al. Brain size and white matter content of cerebrospinal tracts determine the upper cervical cord area: evidence from structural brain MRI. Neuroradiology 2013;55(8):963–70.
[50] Cohen-Adad J, Alonso-Ortiz E, Abramovic M, Arneitz C, Atcheson N, Barlow L, et al. Open-access quantitative MRI data of the spinal cord and reproducibility across participants, sites and manufacturers. Sci Data 2021;8(1):219.
[51] Smith SS, Stewart ME, Davies BM, Kotter MRN. The prevalence of asymptomatic and symptomatic spinal cord compression on Magnetic resonance imaging: a systematic review and meta-analysis. Global Spine Journal 2021;11(4):597–607.
[52] Bédard S, Karthik EN, Tsagkas C, Pravatà E, Granziera C, Smith A, et al. Towards contrast-agnostic soft segmentation of the spinal cord. Med Image Anal 2025;101:103473. https://doi.org/10.1016/j.media.2025.103473.
[53] Karthik EN, Valošek J, Farner L, Pfyffer D, Schading-Sassenhausen S, Lebret A, et al. SCIsegV2: a universal tool for segmentation of intramedullary lesions in spinal cord injury [Internet]. arXiv [cs.CV] 2024. Available from: http://arxiv.org/abs/2407.17265.
[54] Karthik EN, Valosek J, Smith AC, Pfyffer D, Schading-Sassenhausen S, Farner L, et al. SCIseg: automatic segmentation of T2-weighted intramedullary lesions in spinal cord injury. MedRxiv 2024. https://doi.org/10.1101/2024.01.03.24300794.
[55] Cadotte DW, Cadotte A, Cohen-Adad J, Fleet D, Livne M, Wilson JR, et al. Characterizing the location of spinal and vertebral levels in the human cervical spinal cord. AJNR Am J Neuroradiol 2015;36(4):803–10.
[56] Bédard S, Bouthillier M, Cohen-Adad J. Pontomedullary junction as a reference for spinal cord cross-sectional area: validation across neck positions. Sci Rep 2023;13(1):13527.
[57] Valošek J, Mathieu T, Schlienger R, Kowalczyk OS, Cohen-Adad J. Automatic segmentation of the spinal cord nerve rootlets. Imaging Neurosci 2024;2:1–14.
[58] Lord EL, Alobaidan R, Takahashi S, Cohen JR, Wang CJ, Wang BJ, et al. Kinetic magnetic resonance imaging of the cervical spine: a review of the literature. Global Spine J 2014;4(2):121–8.
[59] Valošek J, Labounek R, Horák T, Horáková M, Bednařík P, Keřkovský M, et al. Diffusion magnetic resonance imaging reveals tract-specific microstructural correlates of electrophysiological impairments in non-myelopathic and myelopathic spinal cord compression. Eur J Neurol 2021;28(11):3784–97.
[60] Vallotton K, David G, Hupp M, Pfender N, Cohen-Adad J, Fehlings MG, et al. Tracking white and gray matter degeneration along the spinal cord axis in degenerative cervical myelopathy. J Neurotrauma 2021;38(21):2978–87.
[61] Vallotton K, David G, Hupp M, Pfender N, Cohen-Adad J, Fehlings MG, et al. Tracking White and Gray Matter Degeneration along the Spinal Cord Axis in Degenerative Cervical Myelopathy. J Neurotrauma 2021;38(21):2978–87.
[62] Valošek J, Bednařík P, Keřkovský M, Hluštík P, Bednařík J, Svatkova A. Quantitative MR markers in non-myelopathic spinal cord compression: a narrative review. J Clin Med Res 2022;11(9):2301.